Journal of Molecular Catalysis A: Chemical 383–384 (2014) 58–63

Contents lists available at ScienceDirect

Journal of Molecular Catalysis A: Chemical

journal homepage: www.elsevier.com/locate/molcata

Liquid phase oxidation of diphenylmethane to benzophenone with molecular oxygen over nano-sized Co–Mn catalyst supported on calcined Cow bone

B.H. Monjezi, M.E. Yazdani, M. Mokfi, M. Ghiaci *

Department of Chemistry, Isfahan University of Technology, 8415683111 Isfahan, Iran

ARTICLE INFO

Article history:
Received 17 September 2013
Received in revised form
11 November 2013
Accepted 14 November 2013
Available online 26 November 2013

Keywords:
Cobalt
Manganese
Cow bone
Benzophenone
Diphenylmethane

ABSTRACT

A well-dispersed Co–Mn catalyst immobilized on calcined Cow bone was synthesized and used, for the first time for the selective synthesis of benzophenone by liquid phase oxidation of diphenylmethane under various reaction conditions. The catalyst was characterized using techniques such as UV–vis, SEM, TEM and BET. The catalyst has shown an excellent activity (87%), selectivity to diphenyl ketone (90%) and stability under solvent free conditions. To investigate the leaching of the metals from the support, results of the original and reusable catalyst was correlated and compared, and the catalytic activity of washed catalyst was also demonstrated. Based on the all catalytic results for this reaction, the new catalyst was found to be a highly active and environmentally friendly solid catalyst and has superior catalytic activity.

1. Introduction

Oxidation is one of the most fundamental transformations in organic chemistry and selective oxidation of diphenylmethane (DPM) to benzophenone is an industrially important synthetic process. Benzylic oxidation is the foundation of many current important industrial and fine-chemical processes, as the product benzophenone is known as a component of many consumer products. Benzophenone is primarily used as a photo initiator and fragrance enhancer. It is also used as an ultraviolet curing agent in sunglasses and ultraviolet curable ink. It is also used as an ultraviolet absorber, to block UV-B, UV-A and UV-C radiation, perfume fixative in soaps, flavor ingredient, and polymerization inhibitor for styrene, additive for plastics, coatings and adhesive formulations, in the manufacture of insecticides, agricultural chemicals, hypnotics, antihistamines, and other pharmaceuticals.

It is usually synthesized by the Friedel–Crafts acylation of benzene with benzoyl chloride in the presence of $AlCl_3$. Other processes for the production of benzophenone contain atmospheric oxidation of diphenymethane and decarboxylation of *o*-benzoylbenzoic acid over copper catalysts [1], and oxidation of diphenylmethane using stoichiometric quantities of oxidizing agents like $KMnO_4$ [2], SeO_2 [3] or CrO_3–SiO_2 [4]. Alternatively, benzophenone is also produced by the reaction of benzene with carbon tetrachloride followed by hydrolysis of the resulting diphenyldichloromethane and the oxidation of DPM in the presence of chromic acid and nitric acid [5].

In the above processes, a large amount of waste produced and the usage of stoichiometric amount of catalyst makes the process unacceptable. Also difficult operational problems such as corrosion, the usage of large amounts of catalyst, separation and recovery, deactivation via the aggregation of metal nanoparticles formed in situ during the reaction, disposal of used catalyst, high toxicity, and catalyst removal from the product are other drawbacks.

Homogeneous catalysts are most active catalysts, with many attractive properties such as high chemo- and regioselectivity and high activities. In order to overcome the difficulties of a homogeneous system, the development and utilization of a solid catalyst is important. Recently there has been increased interest in the development of processes mediated by heterogeneous catalysts [6–8] that is one of the best options to overcome these drawbacks. They have excellent stability, are easily accessible, and most importantly, they can be easily separable from the reaction mixture. However, they do have some drawbacks, first, inferior catalytic performance relative to their homogeneous counterparts, because of reduced contacts between catalyst and substrates and second drawback is the use of filtration to isolate the catalyst from reaction mixture, which reduces the efficiency of the system at each cycle. Clark et al. [9] reported the first heterogeneous oxidation of diphenylmethane to benzophenone over alumina supported chromium and manganese.

* Corresponding author. Tel.: +98 3113913254; fax: +98 3113912350.
E-mail addresses: mghiaci@cc.iut.ac.ir, mehranghiaci@gmail.com (M. Ghiaci).

1381-1169/$ – see front matter © 2013 Elsevier B.V. All rights reserved.
http://dx.doi.org/10.1016/j.molcata.2013.11.019

Nanoparticles show very interesting and useful properties in comparison with bulk materials and they have more application and efficiency than micro-scale materials. Nano-catalysis can be considered as a bridge between homogeneous and heterogeneous catalysis. Because of nano-size, i.e., high surface area, the contact between reactants and catalyst increases dramatically and they can operate in the same manner as homogeneous catalysts, at the same time, due to their insolubility in the reaction media, they can be separated out easily from the reaction mixture.

In the last two decades, for selective oxidation of diphenylmethane different research groups have used heterogeneous catalysts such as $KMnO_4$ impregnated on alumina [10], $KMnO_4$ supported on montmorillonite K10 [11], cobalt substituted silicate xerogel and N-hydroxyphthalimide-acridine yellow-Br_2 system [12,13], manganese(III) Schiff base complex [14], metal incorporated molecular sieves (M-MCM-41 where M is Ti, V, Cr) [15], cobalt doped mesoporous TiO_2 (Co/$MTiO_2$) [16,17], Mn–Mg–Al [18], Ru–Co–Al [19], and more recently cobalt porphyrin on CeO_2@SiO_2 [20], CrSBA-15 [21]. Probably to prepare most of the reported catalysts, one should spend a lot of time and efforts, and even uses expensive raw materials. More importantly, for selective oxidation of diphenylmethane, most of these catalysts are not environmental friendly catalysts.

Bone inorganic composition is formed from carbonated hydroxyapatite. Hydroxyapatite (HAP) is a phosphate mineral that having stability, and because of its high adsorption capacity has intrigued much attention as support for transition metal catalysts in various reactions. Structure of pure hydroxyapatite is very similar to hydroxyapatite of bone but there are tiny differences between those due to presence of other ions such as iron in structure of bone hydroxyapatite. In continuation of our research in the field of modifying solid supports and exploring new supports [22], in this work we have synthesized a heterogeneous hybrid Co/Mn nano catalyst on a cheap support, i.e., calcined bone and used it for preparation of benzophenone by liquid-phase oxidation of diphenylmethane with oxygen as the greenest oxidant. The oxidation of diphenylmethane has been carried out in different conditions by monitoring parameters such as time, temperature, amount of catalyst, pressure of oxygen gas, and reusability.

2. Experimental

The reactor and procedures have been previously described [23]. The source of chemicals is Merck chemical company. The cobalt and manganese salts were the (+II) nitrate hexahydrates.

A BEIFEN 3420 gas chromatograph equipped with a FID detector was used to identify the reaction products. The column was a 30 m HP-FFAP with 0.32 mm i.d. and 0.5 μm film thickness. The initial temperature was 170 °C for 5 min. The GC was then ramped at 10 °C/min to 280 °C, and hold for 1 min at that temperature. The products of the oxidation of diphenylmethane were identified by GC/MS (Fisons Instruments 8060, USA).

Scanning electron micrographs were obtained using a Cambridge Oxford 7060 Scanning Electron Microscope (SEM) connected to a four-quadrant back scattered electron detector with resolution of 1.38 eV. The samples were dusted on a double sided carbon tape placed on a metal stub and coated with a layer of gold to minimize charging effects.

A high-resolution Hitachi S4160 field emission scanning electron microscope equipped with an EDX system was utilized in the scanning electron microscopy (SEM/EDS) measurements. The supported catalyst sample was conserved under nitrogen atmosphere. The microstructure and surface morphology of the supported catalysts were characterized by scanning electron microscopy (SEM) method.

Particle size and morphology were evaluated from the transmission electron microscopy (TEM) images obtained in a JEM 2100F microscope operated with an accelerating voltage of 200 kV. The standard procedure involved dispersing 4 mg of the sample in ethanol in an ultrasonic bath for 15 min. The sample was then placed on a Cu carbon grid where the liquid phase was evaporated.

BET surface area and pore size distribution were measured on a Micromeritics Digisorb 2600 system at −196 °C using N_2 as adsorbate. Before measurements, the samples were degassed at 450 °C for 3 h under vacuum (0.1333 Pa).

2.1. Preparation of the bone supported catalyst by osmosis method

In the first step, 450 mL aqueous solution of $Co(NO_3)_2{\cdot}6H_2O$ (0.01 M) was added to 50 mL of an aqueous solution of $Mn(NO_3)_2{\cdot}6H_2O$ (0.01 M). Co/Mn molar ratio was 10:1 in the resultant solution. Pieces of Cow bone were cleaned, piecemealed and were put into the resultant solution for a period of one week. After one week, the pieces of the bone were extracted from the solution. We expected that cobalt and manganese were loaded on the support. Attained sample was dried at 100 °C, and finally calcined at 700 °C for 24 h (Co/Mn-$BSO_{0.01}$).

2.2. Catalytic experiments

According to the optimized reaction conditions, the appropriate amount of diphenylmethane, and solid catalyst were added to a titanium batch reactor. The correct pressure was provided with oxygen (99.98%) and the desired temperature selected. After the reaction, the reactor was cooled to room temperature and the mass balances were calculated from the weights of the reaction mixture before and after the reaction. In the next step, the solid precipitate which mainly consists of catalyst was separated by centrifugation. After addition of *n*-decane as internal standard to the organic phase, the reaction mixture was analyzed by GC and the products were identified by GC–MS.

3. Results and discussion

3.1. Characterization of the catalyst

3.1.1. The Co/Mn immobilized on the Cow bone

In our previous work [22], we have characterized this catalyst which has been prepared by immobilizing cobalt and manganese over calcined bone by osmosis method, and used for oxidation of 2,6-diisopropylnaphthalene.

Nitrogen adsorption–desorption isotherm of the Co/Mn-$BSO_{0.01}$ catalyst is demonstrated in Fig. 1. According to IUPAC categorization [24,25], the Co/Mn-$BSO_{0.01}$ catalyst presented a typical Type IIb nitrogen isotherm with H3 hysteresis loop. The observed hysteresis loop between adsorption and desorption isotherms is associated with differences in the rates of capillary condensation and evaporation. Generally, Type IIb isotherms are obtained with aggregates of plate-like particles, which therefore possess non-rigid slit-shaped pores. Because of delayed capillary condensation, multilayer adsorption is able to proceed on the particle surface until a high p/p^o is reached. Once the condensation has occurred, the state of the adsorbate is changed and desorption curve therefore follows a different path until the condensate becomes unstable at a critical p/p^o. The sharpness of the isotherm and the presence of hysteresis loop at $P/P_0 > 0.7$ illustrates that the catalyst is mostly mesoporous. At low relative pressure, nitrogen adsorption and interaction between nitrogen and partition pores of the catalyst were low. Adsorption of N_2 increases sharply under the high relative pressure because of the capillary condensation within the

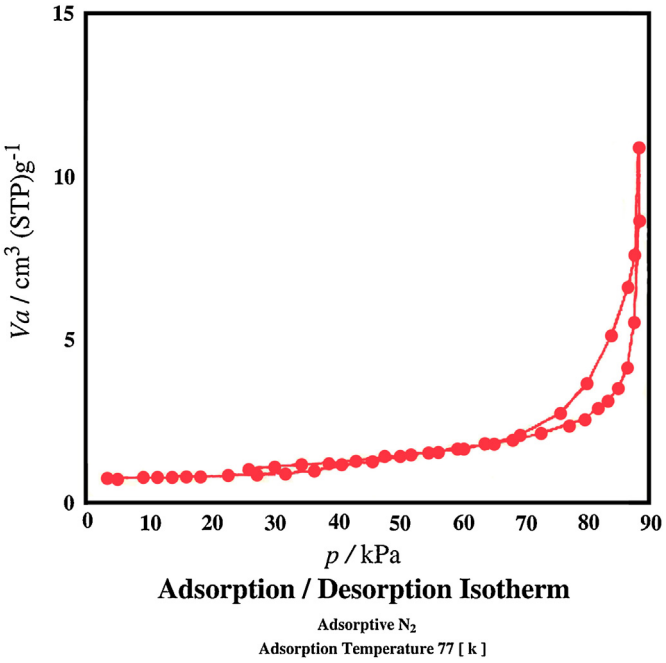

Fig. 1. Adsorption/desorption isotherm of the Co/Mn-$BSO_{0.01}$ nanocatalyst.

Table 1
Textural properties of the Co/Mn-$BSO_{0.01}$ catalyst.

Sample	Co/Mn[a]	S_{BET} ($m^2\ g^{-1}$)[b]	d_{BJH} (nm)[c]	V_{tot} ($cm^3\ g^{-1}$)[d]
Co/Mn-$BSO_{0.01}$	10/1	2.8	3.3	0.63

[a] Molar ratio of metal ions deduced from ICP-AES results.
[b] Brunauer–Emmet–Teller (BET) surface area.
[c] Pore diameter calculated by the Barrett–Joyner–Halenda (BJH) method utilizing the adsorption branches.
[d] Total pore volume calculated as the amount of nitrogen adsorbed at a relative pressure of 0.99.

mesopores of the catalyst. In Table 1, the specific surface area (S_{BET}), total pore volume, and Barrett–Joyner–Halenda (BJH) desorption average pore diameter of the catalyst are reported. BET measurements revealed a low surface area (2.8 $m^2\ g^{-1}$). Even by having a low surface area, oxidation activity of this catalyst was very well. So the active surface sites, related to BET surface area, were significant for the adsorption of diphenylmethane and desorption of the benzophenone molecules.

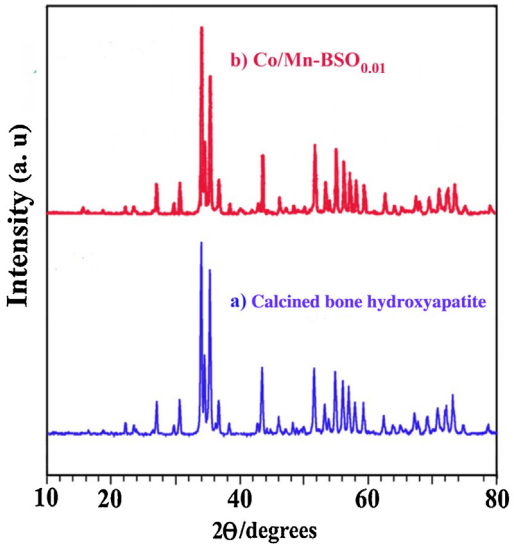

Fig. 2. XRD pattern of (a) calcined bone hydroxyapatite and (b) Co/Mn-$BSO_{0.01}$ nanocatalyst.

3.1.2. XRD data

Fig. 2 shows the powder X-ray diffraction patterns of calcined bone (hydroxyapatite), and Co/Mn-$BSO_{0.01}$ catalyst. Both powder XRD patterns were very similar. Identification of the phases was realized by comparing the experimental XRD pattern to standards compiled by the International Centre for Diffraction Data (ICDD). Sharp peak intensity and well resolved peaks in XRD patterns of the powders at high calcinations temperature proves complete crystallization of the powder. It is clear that the main phase of Co/Mn-$BSO_{0.01}$ nano-catalyst is hydroxyapatite because the amount of nano-catalyst is very low.

3.1.3. SEM and TEM images

The SEM micrographs of calcined bone powder (Fig. 3) were soft agglomerated fine HAP particles. The image shows that the sample is consisted of particles with diameter of 100–500 nm. SEM/EDX mapping indicated a content of nano-particles throughout the catalyst pores that these were related to Co and Mn. Representative TEM images of the Co/MN-$BSO_{0.01}$ catalyst are demonstrated in Fig. 4. Formation of the Co and Mn nano-particles over bone support was confirmed by TEM images. The average size of the nano-particles was estimated to be 2–5 nm for the Co/Mn-$BSO_{0.01}$ catalyst. The cobalt and manganese contents of the bone and the supported catalyst sample were determined by ICP-AES. The molar ratio of the

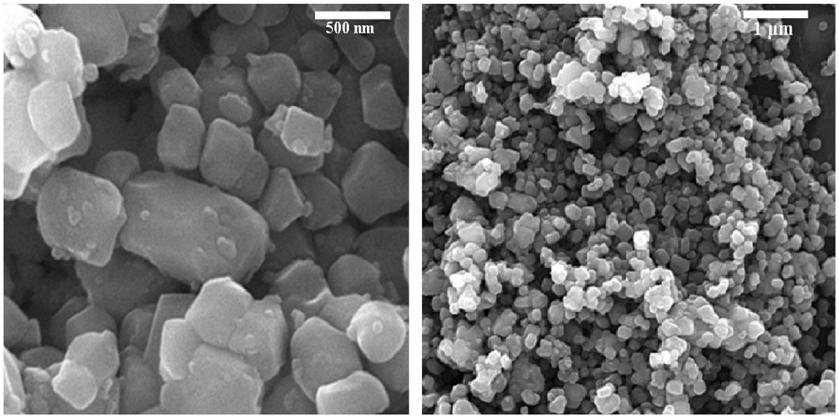

Fig. 3. SEM images of the Co/Mn-$BSO_{0.01}$ nanocatalyst.

Table 2
Analytical data of the catalyst and support.

Catalyst (1 g)	Analysis (mmol)										
	Ca	Na	Mg	Li	K	Sr	Fe	Se	B	Co	Mn
BSO[a]	7.77	0.26	0.24	0.068	0.021	0.015	0.013	0.010	0.007	0.000	0.000
Co/Mn-$BSO_{0.01}$										0.169	0.017

[a] Calcined Cow bone.

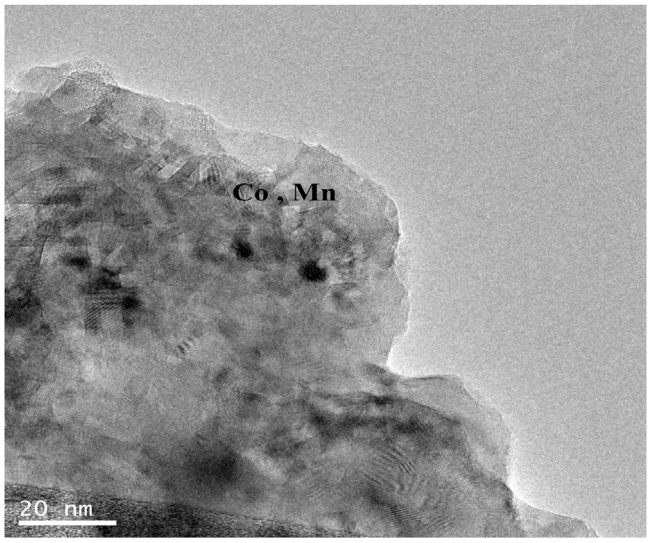

Fig. 4. TEM image of the Co/Mn-$BSO_{0.01}$ nanocatalyst.

measured Co and Mn contents in the supported catalyst sample was 10:1. The ions contents of the initial bone and the Co/Mn-$BSO_{0.01}$ catalyst are reported in Table 2.

3.1.4. DR UV–vis spectroscopy

UV–vis spectra were recorded with aim to reveal changes in the chemical structure of the hydroxyapatite upon immobilization of nano-particles, and also to provide further evidence on the morphology of metal ions. UV–vis spectra of the support and the catalyst are shown in Fig. 5. There should be bands in the region between 300 and 400 nm, which is typical of Co^{3+} octahedral species, as well as a few absorption bands around 543, 580, and 630 nm, which is typical of Co^{2+} ions in tetrahedral coordination. Also bands with similar positions (350–460 nm) have been expected for manganese in the calcined bone environment, which could be interpreted as being an evidence of the presence of tetrahedrally coordinated Mn^{2+} in the framework.

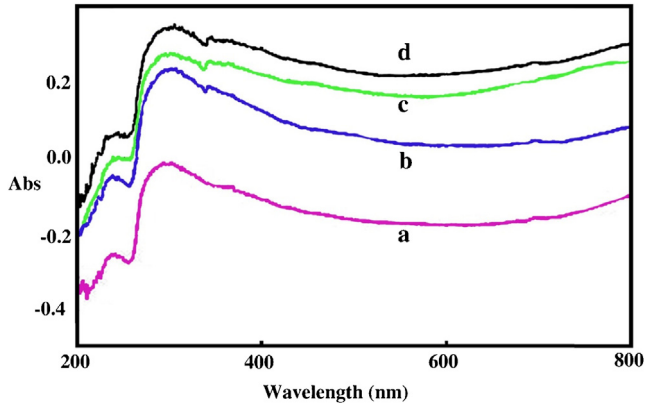

Fig. 5. UV–vis spectra of (a) bone, (b) bone containing Mn, (c) bone containing Co, and (d) bone containing Co and Mn.

3.2. Catalytic performance

The performance of the Co/Mn-$BSO_{0.01}$ catalyst was tested in diphenylmethane oxidation without the need of any solvent and reducing reagent at 353 K. Oxygen was used as the best oxidant. The results of the % selectivity to benzophenone and % conversion of diphenylmethane are presented in Table 3. The conversion and selectivity were monitored by GC analysis. Products were identified by considering their GC–MS and by comparison with the GC of the authentic samples. The oxidation takes place on the alpha-carbon of the alkylbenzene. Formation of the products benzophenone, **1**, and benzoic acid, **2** are illustrated in Scheme 1. It is remarkable to mention that no oxidation was observed in the aromatic ring of the diphenylmethane. The catalyst activity of the solid catalyst was higher in solvent free condition than in the presence of solvent such as CH_3CN.

3.2.1. Effect of temperature

The catalytic activity of Co/Mn-$BSO_{0.01}$ catalyst was investigated as a function of temperature. Table 3 shows the results of the oxidation at 100, 150, 180, and 200 °C. The reaction temperature has a great influence on the progress of the reaction. By increasing the temperature to 200 °C, the conversion increased remarkably. The reaction temperature also affected the distribution of the products and selectivity. By performing the reaction at higher temperature, the selectivity for benzophenone decreases. Therefore, the optimum temperature for the oxidation was chosen at 200 °C.

3.2.2. Effect of pressure of oxygen

Table 3 summarizes the effect of different pressures of oxygen on the oxidation of diphenylmethane over Co/Mn-$BSO_{0.01}$ catalyst at 200 °C. These results showed that the higher conversion was achieved with 17 bars pressure of oxygen as oxidant. In this condition the selectivity of the benzophenone increased to 87% and the conversion increased to 90%. Therefore, the optimum pressure of oxygen for oxidation was chosen 17 bars.

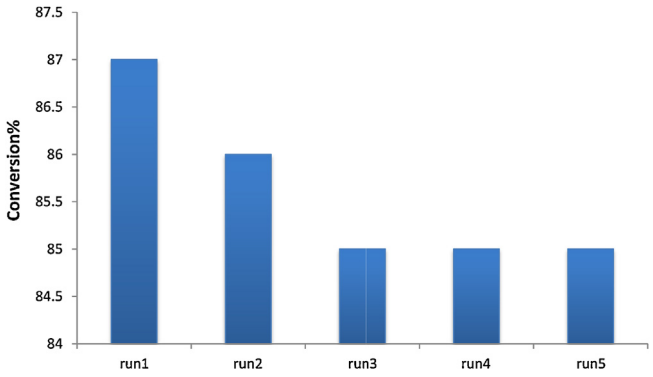

Fig. 6. Reusability of the catalyst at optimum conditions: temperature, 200 °C; pressure of oxygen, 17 bars; amount of catalyst, 100 mg; and time of reaction, 3 h.

Table 3
Effect of the reaction parameters.

Entry	Temperature (°C)	Pressure (bar)	Time (h)	Catalyst (mg)	Conversion %	Selectivity %		
						Benzoic acid	Benzophenone	Others
1	100	17	3	100	21	3.5	95	1.5
2	150	17	3	100	51	6	93	1
3	180	17	3	100	79	9.5	88	2.5
4	200	17	3	100	87	7	90	3
5	200	10	3	100	78	14	80	6
6	200	12	3	100	81	15.5	80.5	4
7	200	15	3	100	79	16	81	3
8	200	17	3	100	87	7	90	3
9	200	17	1	100	21	12	86	2
10	200	17	3	100	87	7	90	3
11	200	17	6	100	89	5	93	3
12	200	17	12	100	90	3	90	7
13	200	17	3	50	81.5	13.5	83.5	3
14	200	17	3	100	87	7	90	3
15	200	17	3	150	85.5	10	87	3

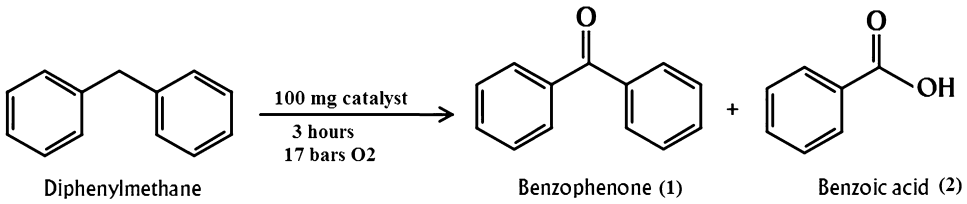

Scheme 1.

Table 4
Catalytic activities of Co/Mn-$BSO_{0.01}$ and some previously reported catalysts in the diphenylmethane oxidation.

Entry	Catalyst	Conversion %	Selectivity %	Oxidant	Reference
1	Co/Mn-SBO	87	90	O_2	This work
2	MnMCM-41	14	100	O_2	[26]
3	MnMCM-48	15	100	O_2	[26]
4	CrMCM-41	51	98	O_2	[27]
5	Ni–Al–hydrotalcite	62	97	O_2	[28]
6	Mn–MgAlhydrotalcite	70	95	O_2	[18]
7	NHPI–acridine yellow–Br_2	65	99	O_2	[13]
8	MnO_4−1 exchanged MgAlhydrotalcite	27	100	O_2	[29]
9	CuMgAl-13	95	100	TBHP	[30]
10	$RuCl_2(PPh_3)3$	75	95	t-BuOOH	[31]
11	CrSBA-15	61	95	TBHP	[20]

3.2.3. *Effect of time*

Table 3 shows the effect of time on the diphenylmethane oxidation with Co/Mn-$BSO_{0.01}$ catalyst. The results show that by increasing the reaction time, the diphenylmethane conversion was increased. By increasing the time of the reaction from 1 h to 3 h, the conversion increased from 21% to 90%, and from 3 h to 12 h almost kept unchanged. Then the optimum time for oxidation was selected 3 h.

3.2.4. *Effect of amount of catalyst*

To study the effect of amount of catalyst, oxidation was carried out at 200 °C, 17 bars, and 3 h. The results are summarized in Table 3. As seen, 100 mg of the catalyst was enough to increase appreciably conversion of the reaction (87%) and selectivity to benzophenone (89%). However, by further increasing of amount of the catalyst, a slight decrease in the conversion was observed. It should be mentioned that in the absence of the catalyst, the oxidation reaction was very poor.

3.2.5. *Reusability of the catalyst*

The catalytic stability of the catalyst in the oxidation of diphenylmethane is shown in Fig. 6. By just separating the catalyst from the reaction mixture by centrifugation, washing it with chloroform and drying at 100 °C the catalyst was used for a new run at the optimum conditions. The activity of the catalyst after at least five runs was approximately steady. We have reported in our previous work [23], that this catalyst did lose its activity after the first run. But it should be mentioned that the medium of that oxidation reaction was acetic acid, and deactivation of the catalyst was attributed to leaching of the catalyst from the support. However, in the oxidation of diphenylmethane which has been conducted in a solvent free conditions, and on the basis of ICP measurements the leaching was not the case.

4. Conclusion

In this investigation, the preparation and characterization of a new heterogeneous nano-catalyst with excellent properties have been described. The synthesized nano-catalyst was characterized by XRD, UV–vis, BET, TEM, and SEM techniques. In summary, the new catalyst could catalyze the oxidation of diphenylmethane to benzophenone. A higher yield of benzophenone was obtained by optimizing of temperature, time, and the amount of nano-catalyst and pressure of oxygen. Under the optimized conditions, a maximum of 87% diphenylmethane with 90% selectivity was achieved.

The data in Table 4 compares the results obtained over Co/Mn-$BSO_{0.01}$ catalyst and other catalysts used for this reaction. As shown in Table 4, the catalyst used in the present study might be one of the best catalysts in respect of oxidation of diphenylmethane to benzophenone. The extension of application of this nano-catalyst to different oxidation reactions is currently under investigation in our laboratory.

Acknowledgments

Thanks are due to the Iranian Nanotechnology Initiative and the Research Council of Isfahan University of Technology and Centre of Excellence in the Chemistry Department of Isfahan University of Technology for supporting this work.

References

[1] S. Kuhn, Nippon Shokukai Kagaku, Jap. Patent No. 59,219,248 (1983).
[2] R. Gopalan, R.W. Sugumar, Ind. J. Chem. 16A (1978) 198–201.
[3] N.D. Valechha, A. Pradhan, J. Ind. Chem. Soc. 61 (1984) 909–911.
[4] S.D. Borkar, B.M. Khadilkar, Synth. Commun. 29 (1999) 4295–4298.
[5] Y. Ogata, H. Tezuka, T. Kamei, J. Org. Chem. 34 (1969) 845–847.
[6] Y. Ono, J. Catal. 216 (2003) 406–415.
[7] H. Hattori, Appl. Catal. A: Gen. 222 (2001) 247–259.
[8] D. Kishore, S. Kannan, Green Chem. 4 (2002) 607–610.
[9] J.H. Clark, A.P. Kybett, P. London, D.J. Macquarrie, K. Martin, J. Chem. Soc. Chem. Commun. (18) (1989) 1355–1356.
[10] A. Oussaid, A. Loupy, J. Chem. Res. (S) (9) (1997) 342–343.
[11] A. Shaabani, A. Bazgir, F. Teimouri, D.G. Lee, Tetrahedron Lett. 43 (2002) 5165–5167.
[12] M. Rogovin, R. Neumann, J. Mol. Catal. A: Chem. 138 (1999) 315–318.
[13] X. Tong, J. Xu, H. Miao, J. Gao, Tetrahedron Lett. 47 (2006) 1763–1766.
[14] H.R. Mardani, H. Golchoubian, J. Mol. Catal. A: Chem. 259 (2006) 197–200.
[15] R.K. Jha, S. Shylesh, S.S. Bhoware, A.P. Singh, Micropor. Mesopor. Mater. 95 (2006) 154–163.
[16] F. Chang, W. Li, F. Xia, Z. Yan, J. Xiong, J. Wang, Chem. Lett. 34 (2005) 1540–1541.
[17] L. Tang, B. Li, Z. Zhai, J. Li, E. Ou, J. Wang, Catal. Lett. 121 (2008) 63–69.
[18] S.K. Jana, Y. Kubota, T. Tatsumi, J. Catal. 247 (2007) 214–222.
[19] T. Matsushita, K. Ebitani, K. Kaneda, Chem. Commun. (3) (1999) 265–266.
[20] M. Selvaraj, D.W. Park, S. Kawi, I. Kim, Appl. Catal. A: Gen. 415 (2012) 17–21.
[21] X. Guo, Y. Li, D. HuaShen, Y. Song, X. Wang, Z. Liu, J. Mol. Catal. A: Chem. 367 (2013) 7–11.
[22] A.M. Ghahfarrokhi, P. Moshiri, M. Ghiaci, Appl. Catal. A: Gen. 456 (2013) 51–58.
[23] M. Ghiaci, M. Mostajeran, A. Gil, Ind. Eng. Chem. Res. 51 (2012) 15821–15831.
[24] S. Brunauer, P.H. Emmett, E. Teller, J. Am. Chem. Soc. 60 (1938) 309–319.
[25] E.P. Barrett, L.G. Joyner, P.P. Halenda, J. Am. Chem. Soc. 73 (1951) 373–380.
[26] N.N. Tusar, S.C. Laha, S. Cecowski, I. Arcon, V. Kaucic, R. Glaser, Micropor. Mesopor. Mater. 146 (2011) 166–171.
[27] S.E. Dapurkar, H. Kawanami, T. Yokoyama, Y. Ikushima, Catal. Commun. 10 (2009) 1025–1028.
[28] S.K. Jana, P. Wu, T. Tatsumi, J. Catal. 240 (2006) 268–274.
[29] V.R. Choudhary, J.R. Indurkar, V.S. Narkhede, R. Jha, J. Catal. 277 (2004) 257–261.
[30] D. Kishore, A.E. Rodrigues, Catal. Commun. 10 (2009) 1212–1215.
[31] S.I. Murahashi, N. Komiya, Y. Oda, T. Kuwabara, T. Naota, J. Org. Chem. 65 (2000) 9186–9193.